16th International Learning & Technology Conference 2019

Thin Vessel Detection and Thick Vessel Edge Enhancement to Boost Performance of Retinal Vessel Extraction Methods

Mohammad A.U. Khan[a,c], James Carmichael[b], Akila Sarirete[c], Nighat Mir[c*],

[a]*Al Ghurair University, P.O. Box 37374, Dubai, U.A.E.*
[b] *University of Modern Sciences, P.O. Box 231931, Dubai, U.A.E.*
[c] *Effat University, P.O. Box 34689 , Jeddah 21478, Saudi Arabia*

Abstract

Abnormal changes in the geometry of retinal blood vessels are often key indicators for a range of ocular pathologies. Currently, the detection of such pathological changes is largely a manual labor-intensive process that must be performed by expert clinicians to ensure correct diagnosis. Although there have been previous efforts to automate such diagnostic procedures using computer-aided diagnostic (CAD) applications, these computerized methods sometimes lack the necessary sensitivity to detect blood vessels which are of low contrast, i.e. blood vessels which are not easily distinguished from their surrounding background. In order to improve CAD detection of low contrast blood vessels, a specialized filter construction is proposed with functionality that can be implemented as an add-on module to enhance the performance of existing CAD blood vessel detector applications. The improved low-contrast detection capability of the specialized filters has been validated by a series of tests which demonstrate that the proposed technique outperforms other state-of-the-art CAD applications when processing retinal fundus images extracted from publicly available image databases.

Keywords: Thin Vessels; CAD; Triple-Stick Filter; Low-Contrast Detection.

1. Introduction

Unexpected changes in the size and shape of retinal blood vessels are often precursors to certain ocular pathological conditions such as diabetic retinopathy (DR) and maculopathy [1]; these ocular diseases are themselves indicators of more serious generalized disorders such as hypertension, diabetes, and stroke [1]. Currently, the analysis of retinal images – also known as *fundus* images – is largely a manual labor-intensive process requiring the input of expert

clinicians to effect a correct diagnosis. Fortunately, the procedures involved in fundus image analysis can be facilitated by the use of computer-aided diagnostic (CAD) applications, particularly those CAD systems which use automated feature segmentation methods in order to highlight blood vessel networks in retinal images [2]. The production of retinal fundus images normally requires the use of specialized cameras - known as fundus cameras – that are used to capture high-resolution photographs of the interior surface of the eye, inclusive of the retina, retinal vasculature, optic disc, macula, and posterior pole. The processing of fundus images to highlight the vascular networks therein can provide useful diagnostic information since – as mentioned previously – ocular pathological conditions are often heralded by various geometric changes in the diameter, length and branching angle of retinal blood vessels [3]. Conversely, certain types of ocular pathology diagnostic procedures – such as those which test for *exudates* (i.e. abnormal masses of cells and fluid found close to retinal blood vessels) or microaneurysms [4] – require the removal of vascular network details from the fundus image. Moreover, since retinal vascular network patterns are as individual-specific as fingerprints, they can also serve as a means of biometric identity identification [5].

As a relatively new sub-discipline in the field, computerized image processing procedures for the detection and analysis of ocular vascular networks are still faced with several challenges, including (a) the presence of image noise, (b) low contrast between a given retinal blood vessel and its surrounding background, and (c) substantial variations in the width of blood vessels within the same vascular network. In addition to the foregoing, there is also the possibility that the presence of pathological manifestations such as overlapping lesions and exudates may mistakenly be identified as blood vessels [6].

In order to minimize image processing errors, a variety of filtering techniques have been devised to detect and highlight blood vessels in retinal images, including a recent innovation whereby a computationally simple geometric filter - known as a fixed-scale line detector - has been proposed in which a network of one pixel- wide lines are superimposed on a rectangular background; the multiple points of intersection created by these thin lines and any underlying blood vessels produce the cumulative effect of intensifying the contrast between a given blood vessel and its immediate background, even if the background manifests conditions of varying brightness [7]. As a further refinement, Nguyen et. al. [8] report improvements on the performance of fixed-scale line detectors by using a multi-scale approach wherein lines of varying lengths (instead of fixed lengths) are superimposed on the image background, this variable-line-length method has resulted in the reduction of pixel shadows which tend to occur when a fixed-scale line intersects with two blood vessels that are in relatively close proximity to each other. Subsequent investigations [9] have shown that improved vascular segmentation is achieved by using lines generated from the application of weighted linear algorithms as opposed to earlier multi-scale methods.
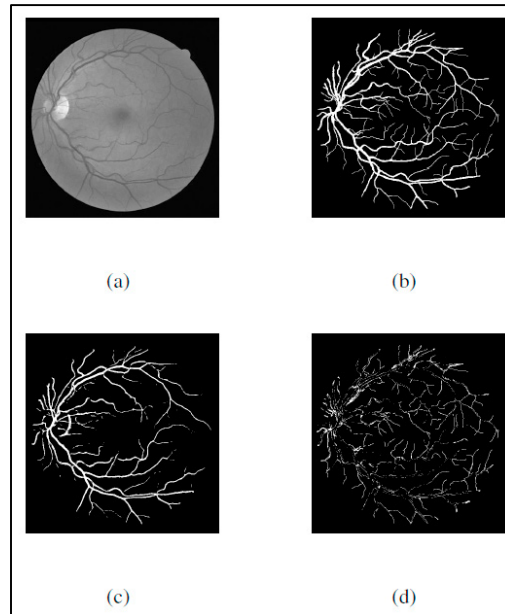
Fig. 1. Analysis of Multi-scale line filtering output: (a) shows a green channel of fundus image, and (b) depicts the ground truth segmentation done manually, (c) shows the segmented output produced by multi-scale line filtering and (d) shows the undetected blood vessels resulting from the multi-scale line filtering approach in (c).

Despite the commendable efforts of previous research groups to achieve these incremental improvements in vessel segmentation accuracy, it is the opinion of this research team that the current state-of-the-art multi-scale line detectors have not yet realized their full potential. In an attempt to assess the current effectiveness of industry-standard multi-scale line detectors, a software application incorporating a variant of the multi-scale technique was used to detect and extract blood vessel network features from a retinal image which had previously been manually processed for the extraction of "ground truth" vascular segmentation data. The results (displayed in Fig. 1) of the multi-scale line detector processing revealed two major limitations, which are as follows:

Firstly, the detector's segmentation accuracy is substantially less effective at detecting the edges of blood vessels as compared to identifying their central regions; this discrepancy is particularly evident in the case of thicker blood vessels of much larger width than the one-pixel-wide detection lines used by multi-scale detectors. It would seem that this problem is mainly due to the fact that the segmentation accuracy of a multi-scale line detector is dependent on contrast between the vessel and its surrounding background, thus the segmentation accuracy of multi-scale line detectors usually diminish in direct correlation to the reducing levels of contrast which typify the regions around blood vessel edges, making such edges difficult to distinguish from their immediate background. This edge detection problem can be mitigated by applying an enhancement filter – e.g. the improved vessel-ness filter suggested in [10] – which reduces the dependence on contrast by utilizing directionality strength as defined purely in terms of Hessian eigenvalue ratios (such eigenvalues being implemented as a 2 x2 second-order derivative matrix).

The second major limitation is that multi-scale line detectors will occasionally fail to identify the presence of thin blood vessels (i.e. blood vessels that are only one or two pixels in diameter). This difficulty in detecting thin vessels is largely due to the relatively low pixel density of such vessels as well as the fact that the pixels represented by these vessels are often very similar in color and hue to pixels resulting from image noise. Of course, the most obvious solution to this problem would be to increase the contrast of such thin blood vessel pixels so that they are more easily differentiated from adjacent pixels. In an attempt to resolve this issue of thin vessel detection, several recent research efforts have proposed various modified forms of line filters that are specifically designed to exhibit a detection bias towards thin vessels while ignoring larger vessels. An example of such a biased filter is the tramline filter proposed by Hunter et al. [11]; a typical implementation of a tramline filter would consist of three parallel lines,

wherein the middle line is directly superimposed on the targeted blood vessel while the outer two lines are positioned in close proximity on either side of the vessel under scrutiny. Unfortunately, the tramline detection method has not proven to be an adequate solution to the thin-vessel detection problem because it is often the case that thin blood vessels are quite tortuous (i.e. frequently changing orientation along their length). The triple-stick filter [12] attempts to improve upon the Tramline approach by using a nonlinear filter for fissure detection. The triple-stick method differs from the tram-line filter in that the former technique considers the separation distance between the three lines when attempting to isolate a thin vessel. If necessary, a triple-stick filter can adjust the distance between the two outer lines during the process of demarcating a low-contrast blood vessel. Given the ability of the triple-stick approach to vary the distance between the left-most and right-most lines, it was the decision of this research team to implement a solution which incorporates this approach since it is inherently more flexible and capable of coping with blood vessels which are tortuous. Moreover, since this research team has implemented this enhanced triple-stick detector as a type of add-on/plug-in module, it can be integrated into existing multi-scale line detector software applications to boost their accuracy in the context of computerized retinal image segmentation. The following section reviews the work of previous investigations in the domain of retinal image processing.

2. Review of Previous Work

This section provides a brief summary of current state-of-the-art methods for retinal blood vessel segmentation which, in general, fall into four categories, i.e. (i) seed point detection, (ii) matched filter segmentation, (iii) morphological matching and (iv) feature vector analysis. The subsections that follow present detailed descriptions of these four approaches respectively.

2.1 Seed Point Detection

The seed point detection method [13, 14, 15, 16, 17, 18] is based on the selection – either manually or automatically – of a *seed pixel*, i.e., a pixel which is estimated to be within a region of the image representing the center-line of a specific retinal blood vessel; using a process known as region-growing, the pixels immediately surrounding the seed pixel are evaluated to determine if they are similar to the seed in terms of grayscale or color properties. If these neighboring pixels are sufficiently similar, then they are included to form a region of pixels which will expand until encountering a border, i.e. a group of pixels which are classified as a separate region because of substantial dissimilarity. Vlachos et al. [19] employ a multi-scale line-tracking procedure to segment blood vessels starting from a set of seed pixels (determined by the brightness selection rule); the region-growing process will terminate when the pixel brightness cross-sectional profile is no longer valid. After the segmentation procedure has been completed, the image maps at different scales are then combined together to produce a multi-scale image map. Apart from the primary goal of achieving vessel segmentation, the seed pixel method offers the advantage of providing important information about vascular architecture, such as the varying diameters of blood vessels as well as the number and position of vessel branching points within the network. However, a significant disadvantage of the seed detection method is that it typically has limited success in identifying bifurcations and crossover points within any given vascular network. Such failure to detect cross-overs and bifurcations can sometimes cause the seed detection region-growing process to terminate prematurely and thus result in an incomplete segmentation of the vascular network under scrutiny.

2.2 Matched Filter Analysis

This second vascular enhancement technique involves the use of matched filters [20] whereby it is assumed that the intensity profiles for all blood vessel cross-sections will exhibit characteristics of a Gaussian function, thus a set of oriented Gaussian shaped filters with varying orientations is used to evaluate the blood vessel under examination. Using such Gaussian analysis, the maximum response is retained for each pixel processed and these accumulated maximum responses should produce the desired vascular network segmentation. A range of incremental refinements [21, 22, 23, 24] have been proposed which have realized some improvements on the original matched filter technique,

including the use of the threshold probing technique [21], double-sided thresholding [23], and the employment of first order Gaussian derivative methods to improve thresholding [24]; these matched filter methods usually reduce the incidence of *false positives*, i.e. erroneously identifying some non-vascular artifact in the image as a blood vessel. Despite these advances, a fundamental limitation of matched filter methods is the premise that the cross-sectional intensity profile of a blood vessel is generally Gaussian-shaped, which is not always the case. Moreover, matched filter techniques operate on the dubious assumption that blood vessels are *piece-wise linear*, i.e. that any blood vessel can be decomposed into a series of straight lines and that the diameter of each of these linear sub-segments will be constant from end to end. In fact, it is occasionally the case that the width and orientation of any given retinal blood vessel will vary substantially along its length and thus defeat matched filter processing techniques.

2.3 Linear Analysis

The third approach to vascular segmentation is – as is the case with matched filter analysis – also based on the assumption that blood vessels within a network are piece-wise linear and connected. The most widely used implementation incorporating the linear approach is that proposed by Zana et al. [25]. Here, mathematical morphological operators with linear structuring elements are used to enhance and differentiate the vessels from their immediate background. Jiang et al. [26] propose a multi-threshold probing technique to threshold the image at different levels and then employ a verification procedure to detect individual vessels in the segmented images. The final segmentation is obtained by a combination of those segmented images returned by each segmentation iteration. Vermeer et al. [27] use the Laplacian filter and thresholding to enhance and extract blood vessels from retinal images. A method based on morphological closing operators is then applied to enhance the edges of the blood vessel in conditions of central light reflex. In [28], the local maxima over scales of the gradient magnitude and the maximum curvature principle are used as two features to classify each pixel as either vessel or background via a multiple-pass region growing process. Lam et al. [29] employ the image's gradient vector field to detect vessel-like objects while employing the normalized gradient vector field to detect a given blood vessel's center lines (i.e. area between the vessel walls). In order to reduce the likelihood of false positives, a pruning process is applied to exclude all pixels appearing to represent blood vessels but which are unlikely to be such since they are too distant from known vessel centerlines. One of the more advanced algorithms using the piece-wise linear approach has been implemented by Lam et al. [30], wherein three different concavity measures are proposed to detect the presence of blood vessels which may be obscured by bright and dark lesions in an abnormal retina.

2.2 Feature Vector Analysis

The enhancement of vascular networks via the use of machine learning techniques based on feature vector analysis [31, 32, 7, 33, 34, 35, 36, 37, 38] represents yet another approach to the vessel segmentation problem. Essentially, this technique first converts all the pixels in an image into a series of feature vectors. Some form of supervised classifier (e.g. artificial neural networks [21], K-Nearest-Neighbors classifiers [6,22], support vector machines [8,26] or Bayesian classifiers [7]) is used to train the algorithm to classify each input image pixel as either belonging to a blood vessel or the image background. It has been demonstrated that supervised methods (wherein the classifier is trained with manually labelled data) are generally more accurate than their unsupervised counterparts, inclusive of all those methods discussed in the preceding subsections of this literature review. It must be noted, however, that supervised methods require a substantial labor-intensive effort to manually label fundus image training data and such labelled data may not be readily available in typical real-world conditions. Furthermore, supervised methods often require additional labelled data and training iterations to achieve optimal performance when confronted with a corpus of images that has been generated by cameras which did not produce the images from the training data. This inherent need to re-train to achieve optimal performance often discourages clinicians from using feature vector classifiers since there may not be sufficient manpower and resources to annotate sufficient quantities of training data.

It is to be noted that none of the four principal analytical techniques discussed in this literature review has resulted in the implementation of an automated vessel segmentation method which is computationally economical but yet robust and consistent. In many instances, for example, automated segmentation techniques are defeated by low-contrast and/or high noise conditions which make blood vessel detection and enhancement difficult. Vessel bifurcation constitutes yet another feature of vascular networks which has proven to be a challenge for current state-of-the-art

segmentation techniques; Hessian-based segmentation methods are particularly inaccurate when analyzing bifurcation points because Hessian segmentation tends to suppress certain disk-like artefacts which can occur at the point of blood vessel branching; unfortunately, the suppression of such disk-like features normally results in the segmentation result producing a fragmented representation of the vascular network under scrutiny.

3. Proposed Method for Retinal Vessel Extraction

The reader is reminded that the main objective of this investigation is to formulate a method to highlight the presence of thin blood vessels in retinal vascular networks. It must be emphasized that thin vessel enhancement is particularly important for conventional multi-scale line detectors because such detectors tend to perform poorly vis-à-vis detecting the edges of blood vessels. In order to improve the performance of multi-scale detectors, a combined multi-stage method (see Fig. 2) is proposed which will now be detailed in the following stages.
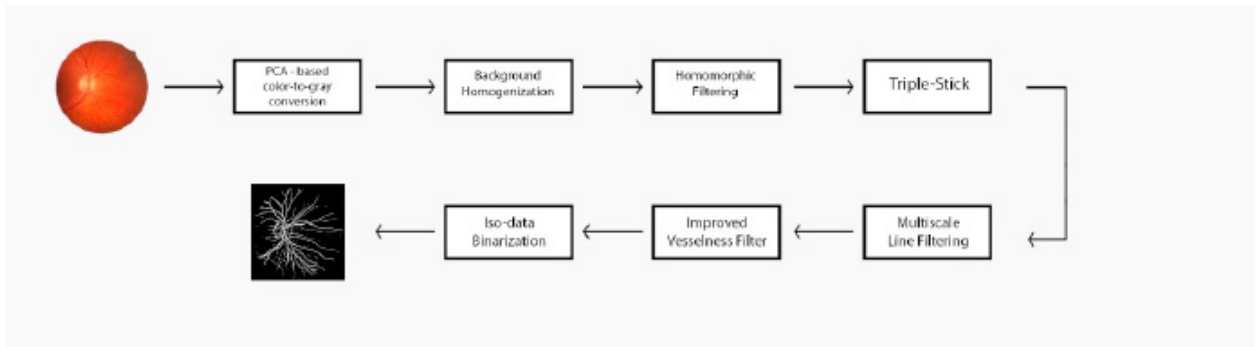

Fig. 2. Block diagram for the proposed Retinal Vessel Extraction method.

1) The first stage is to convert the acquired color fundus image, f, to a grayscale representation. Since the conversion process is variable, (i.e. a given color image may have multiple grayscale representations), it is important to select the grayscale conversion process which would provide optimum contrast between the blood vessels and their immediate background. To this effect, instead of employing the usual grayscale conversion based on green channel sampling, this research team has opted to employ principal component analysis (PCA) as per the findings of a previous research effort in this domain [39]. The conversion process is as follows: firstly, a vectored color image ($f_{rgb} \in R^3$) is created by combining the stacked output of three color channels (i.e., red, green and blue); upon completion of the stacking procedure, a zero-mean YCbCr image ($f_{ycc} \in R^3$) is computed to separate luminance and chrominance channels using the conventional transfer function $f(\cdot)$. The next step is to compute three eigenvalues $\lambda_1 \geq \lambda_2 \geq \lambda_3 \in R^1$ and their corresponding PCA-generated normalized eigenvectors $v_1, v_2, v_3 \in R^2$. The resultant gray image ($f_{gray} \in R^2$) is constructed by the weighted linear combination of three projections as per their eigenvalues. The numerical image data output by these operations is reduced to a single grayscale dimension with values ranging from 0 to 255. It must be emphasized that the derived eigenvalues are used as weighting factors for projection results onto corresponding eigenvectors. As a result of this projection, the color-to-gray mapping is dominated by the first subspace projection, thus the role of the second and third subspace projections is mostly to contribute to preserving details of a color image in a gray image. Fig. 3 visualizes the overall conversion process for an input color image by providing specific examples of the resulting images.
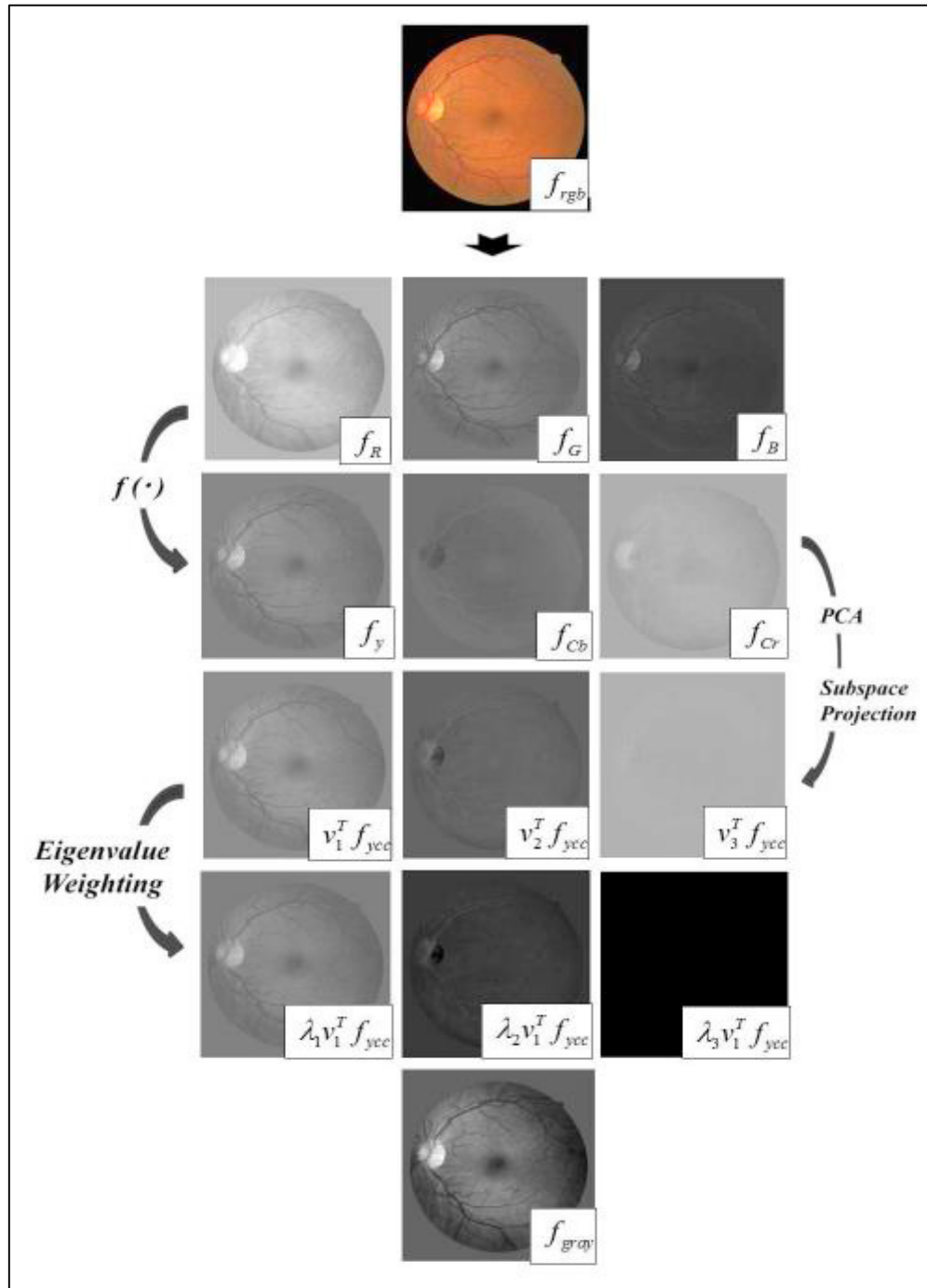
It is apparent that the f_{gray} histogram in Fig. 4(b) contains a wider range of data points compared to the f_{gray} histogram in Fig. 4(a), thus the implication here is that PCA-based color-to-grayscale conversion technique yields more data as compared to methods based on a green channel selection.
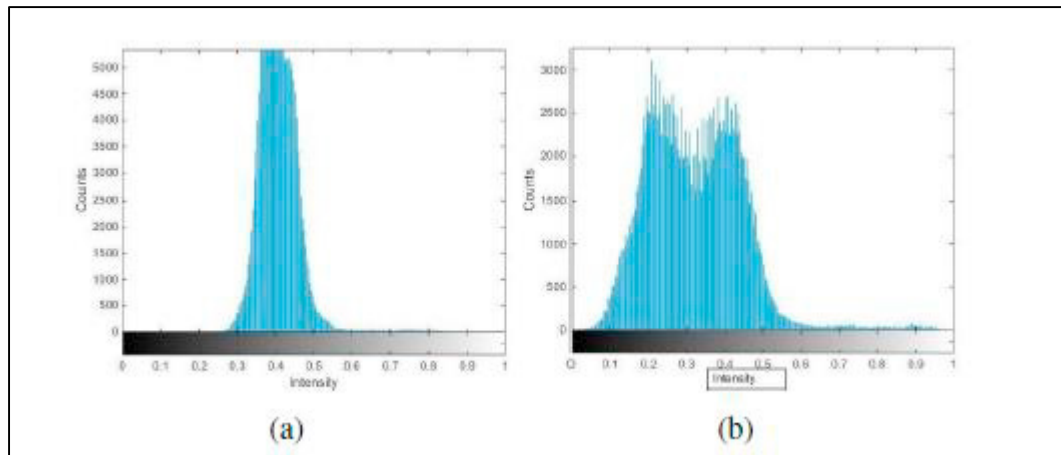
Fig. 4. (a) Histogram of Green channel f_{green} (b) Histogram of PCA-based Grayscale image f_{gray} (x; y).

2) The next phase in the color-to-grayscale conversion process is to ensure that all areas of the image background are of uniform intensity since retinal image backgrounds are often characterized by a gradual variation of intensity which becomes more pronounced at the center of the image, i.e. the central macular area. Of course, variation in image background intensity is to be avoided since such intensity/brightness variation can nullify the effects of any pixel enhancement procedures to increase the contrast of thin blood vessels. In order to eliminate this intensity variation problem, standard homomorphic filtering techniques have been applied whereby non-linear image data are mapped and reduced to a linear domain so that linear filter techniques can be applied to minimize image noise resulting from inconsistent illumination; after the removal of such noise, the image data are mapped back to the original domain. Apart from reducing illumination noise, homomorphic filtering has the added benefit of increasing contrast in low contrast areas of the image.

Given that image rendering techniques for biomedical applications are designed to provide not only image data but also information defining any associated masks describing the image's background and foreground regions, homomorphic filtering techniques – in particular Guillemaud filtering [15] – are often employed to enhance regions of interest (ROI) within such images. In essence, the Guillemaud filter (the architecture of which is depicted in Fig. 5) is a mechanism that uses a *Homomorphic Unsharp Masking* (HUM) algorithm to process one or more ROIs that can be represented as a simplified binary image (such binary images being useful because they suppress a phenomenon known as the *streak artifact* that is often manifested at boundary demarcations separating foreground and background regions within an image). Unfortunately, HUM processing techniques often produce collateral haloes around the edges of the larger blood vessels within a vascular network. In an effort to minimize this halo effect, this research team proposes a modified HUM analysis protocol that we have dubbed as *Halo Compensated Homomorphic Unsharp Masking* (HC-HUM). The HC-HUM approach represents an incremental improvement upon the conventional homomorphic filter since it removes over-illumination artefacts from areas corresponding to the boundary regions of the larger blood vessels in a vascular network. In order to achieve the objective of eliminating halo effects, the HC-HUM performs a gray-level correction on the upper ranges of the selected image's grayscale spectrum by effecting a non-linear gray-level mapping in order to achieve a more nuanced image representation exploiting the full grayscale range (i.e. from '0' to '255'). Based on the results reported in a previous work by some of the members of this research group [30], the contrast-stretching block in the Guillemaud's scheme [22] has been replaced by two blocks devoted to non-linear gray-level mapping to achieve the desired improved grayscale dynamic range. It has been demonstrated by various experimental procedures that when compared to standard HUM filtering techniques the HC-HUM approach is more effective in the context of removing halo effects, as is apparent in Fig. 6.
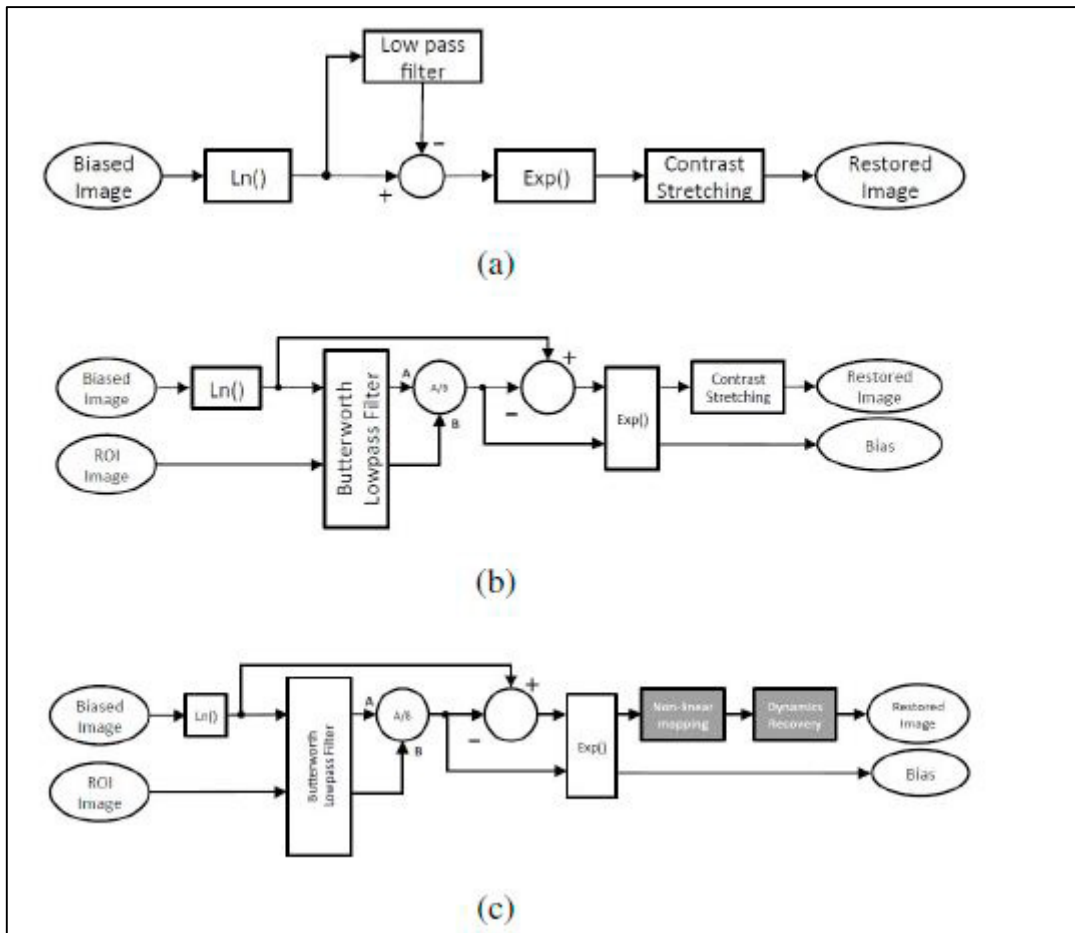
Fig. 5. a) Classic Homomorphic Filtering; (b) Guillemaud Homomorphic Filtering; and (c) Halo Compensated Homomorphic Filtering.

3) After completing HC-HUM processing, the final stage in the vascular network enhancement process is to apply triple-stick filtering techniques to the background of the homogenized grayscale image. It is to be noted that the triple-stick approach has already proven effective in another domain of medical image processing, namely the detection of pulmonary fissures in thoracic CT scans [40]. In the case of triple-stick filtering for thin vessel enhancement, this research team has implemented a series of thin strip decompositions for a given local rectangular neighbourhood of an image under consideration, a nonlinear derivative operator perpendicular to each thin strip is then defined; the standard deviation of the intensity along the main strip is then computed to devise a composed likelihood function which will produce a strong response to the resulting fissure-like bright lines. The application of the composed likelihood function also has the added benefit of suppressing undesired structures such as blobs, step edges, and - in this context - even larger blood vessels which might interfere with the detection of thinner vessels. The successful performance of the filter, as reported in [8], has motivated this research team to utilize said triple-stick filtering techniques for enhancing thin blood vessels in retinal images. As discussed previously, the main challenges associated with the detection of small vessels is that they are usually only one pixel wide in diameter but can vary substantially in structure and shape; these variations are often exacerbated by the presence of high-level imaging noise and interferences from adjacent exudates.

Low-contrast thin vessels are usually represented in digital fundus images as a series of single-pixel wide elongated and fragmented lines which are often mis-classified as instances of image noise by traditional line filtering techniques. In a bid to correct such classification errors, this research team has opted to use the triple-stick filter approach wherein the middle stick is superimposed on the blood vessel's center-line while the left and right sticks are

positioned just outside the vessel boundaries; the three-stick parallelogram-type structure is then rotated on its axis to find the optimal orientation for a series of piece-wise alignments of the blood vessel under scrutiny.   This stick-based smoothing can be considered as a variant of oriented *anisotropic Gaussian* filtering, whereby the long axis scale is much larger than the scale of the short axis. The governing equation for the triple-stick filter is stated in Eq. 1. As displayed in Fig. 7(a), we use μ_M , μ_L, and μ_R to indicate the mean intensity respectively along the middle and the two outer sticks, a nonlinear operator perpendicular to the sticks is defined as:

$$\lambda_\perp^s = \min\,(\mu_M - \mu_L,\, \mu_M - \mu_R). \qquad (1)$$
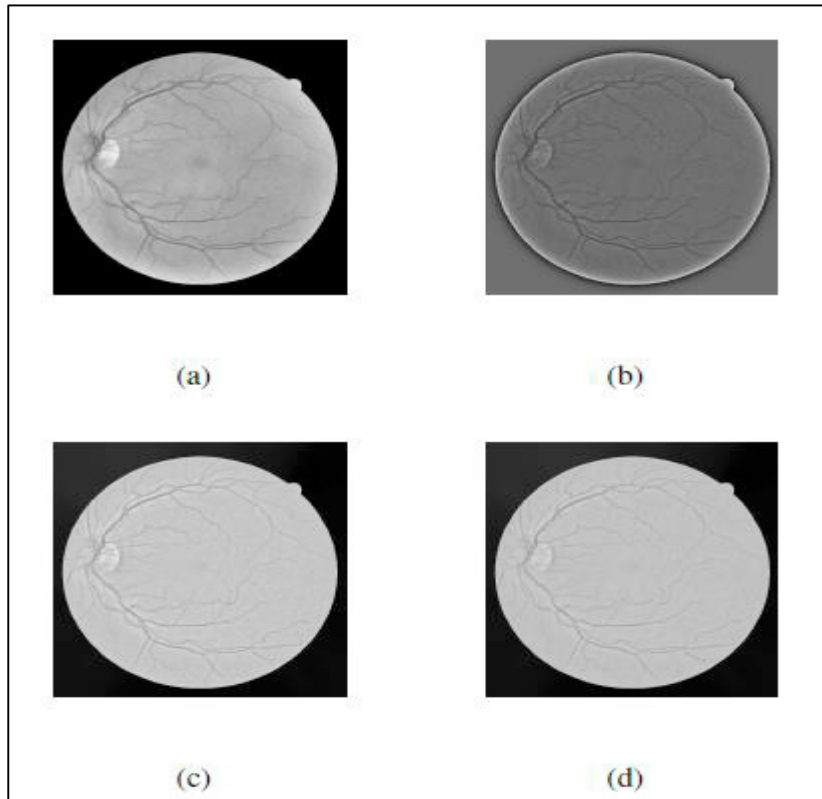

Fig. 6. Background Homogenization. (a) Green Channel Image; (b) Classic Homomorphic Image; (c) Guillemaud Scheme Output Image; and (d) Halo-compensated Homomorphic Image.

The incorporation of a spacing parameter is to render the processing algorithm less sensitive to low intensity regions of the image as well as to enhance the detection of blood vessels with varying width or blurred boundaries. Additionally, due to the sparseness of vessel structure, the adjacent background on both sides of the vessels also takes a low-intensity strip shape. In fact, the utilization of the triple-stick approach to determine the shape and orientation of linear vessels and thus distinguish them from nearby artifacts is an analytical process which is very similar to that used by human experts. Here, the min(.) in Eq.1 is adopted particularly for suppression of step edges, which often correspond to large vessel and optical disk boundaries. Hunter et al. [15] employ a similar scheme by applying tram-line filtering for retinal vessel segmentation. In such circumstances, thin and/or fragmented lines of pixels representing vascular structures will be assigned a high value of $\lambda_\perp^s$. Conversely, wider lines (which normally represent large vessels or step-edges) will be assigned a lower response and therefore not considered during the binarization of the retinal image. In the case of blob-shaped objects, the $\lambda_\perp^s$ will give neither a full nor null response, i.e. the filter will give an incorrect response which can be treated as a background artifact. In order to resolve this problem of false

response to blob-like structures, we introduce another processing operation $\lambda_\parallel^s$ equal to the standard deviation of the pixel intensity along the middle stick. This procedure is similar to the well-established procedures for determining vesselness [17], [18] , $\lambda_\perp^s$ and $\lambda_\parallel^s$ are similar to the Hessian eigenvalues: they also reflect the local contrast in the two principal directions. Accordingly, a 2D vessel likelihood function can then be defined as:

$$\ell^s = \lambda_\perp^s - \kappa \lambda_\parallel^s. \qquad (2)$$

Here, κ is a positive coefficient to suppress the effects of axial intensity inhomogeneity. As per the parameters of Eq. 2, blob-shaped artifacts will evoke a low response since they will exhibit substantial intensity variation along the middle stick of the three-stick filter. The template is rotated in all possible directions to cater for thin vessels of various orientations. Accordingly, we select the stick template with the maximum response as defined by Eq. 2; this maximum response then constitutes the optimal kernel. Thus, the multidirectional information can be integrated with:

$$\ell_m^s = \max (\ell_\theta^s, 0 \leq \theta \leq \pi). \qquad (3)$$

In this context, ℓ_θ^s indicates the linear likelihood estimation of the triple-stick filter output in the θ direction. The enhanced thin-vessel image is then superimposed on the uniform-background image to enhance the low-contrast thin vessels as shown in Fig. 7.
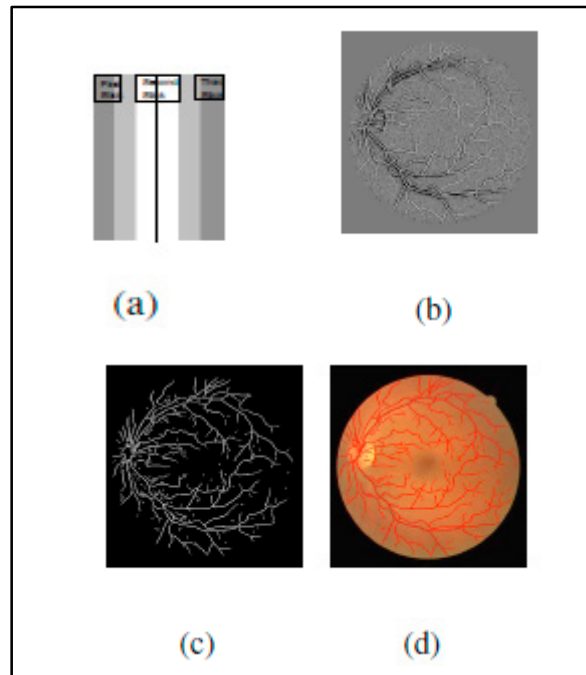

Fig. 7. Thin Vessel Enhancement. (a) Triple-Stick Filter Construction with a wide middle stick and two thinner sticks on the left and right. The middle stick averages the thin vessel pixels, while the left and right stick is used for averaging the background pixels in the neighborhood of the thin vessel; (b) Triple-Stick Filter Output; (c) Marker Image generated from binarization of image data (b); and (d) Overlaying the marker image over the retinal image to show the effectiveness of triple stick filter in extracting thin vessels.

4) Finally, the resulting image featuring thin-vessel enhancement is now ready to be filtered with multi-scale line filters. Multi-scale line filtering is a specialized procedure of more generalized geometric filters. Geometric filters are scalar functions $\nu: \mathbb{R} \Longrightarrow \mathbb{R}$, which selectively amplify a specific local intensity profile in a given sub-region of an image. Several geometric filters have been proposed in previous investigations and the majority of these filters attempt to characterize a specific local structure in an image by analyzing second-order intensity derivatives or Hessians at each point in the image. To enhance any local structures (which may be of variable size), filter-based analysis is typically performed in the Gaussian scale space of the image under scrutiny. However, for the case of retinal images, attempting to classify blood vessels using a second-order Hessian derivative matrix may prove to be impractical due to the presence of noise from nearby non-vasculature structures. The alternative method, therefore, is to employ multi-

scale line filtering techniques since they do not rely on point-wise derivative computations to obtain optimum vessel tree enhancement.

It is to be noted that a line detector is essentially a difference of two local averaging processes, one of these processes being isotropic and the other anisotropic. The isotropic average is along a rectangular region surrounding the pixel of interest, while the anisotropic average is along a directed line with pixel of interest at its center. Since they are directional in nature, line detectors have to be rotated to be aligned with the orientation of the underlying feature in order to provide the best detection score. Since blood vessels are often very tortuous, this research team has opted to use a combination of large and small-scale line detectors (i.e. a multi-scale line detector) to execute vessel segmentation tasks. A line filter of a given length – when convolved with a given input retinal image – will produce a series of scale images and each of these corresponds to the application of a set of a line filter of specific length. In a previous investigation, Nguyen [8] assigned the same weight for each scale (i.e. individual set of line filters); Nguyen's algorithm produces a final response which is essentially the arithmetic addition of line responses from individual line scales that were applied. The response at each image pixel is defined as:

$$R_{combined} = \frac{1}{n_L+1}\left(\sum_L R_W^L + f\right). \quad (4)$$

The problem with the linear-combination analysis proposed by Nguyen is that it assigns equal weight to all scale images produced by the various filters; however, it is evident that some scales are more prominent than others in terms of their contribution to the final result. We therefore propose that the weight of these contributions can be better judged by the reciprocal of the quantum of noise variance which they contribute to the production of the final image. For a given window size, it has been observed that as the line detector's filter line length increases, the corresponding response image becomes less noisy [9]. Given this phenomenon, the noise variance associated with response images can be estimated by taking the difference between the largest-scale line-detection response and individual responses. This difference in response will largely contain noise, and the average squared-amplitude of the difference image provides an estimate of the noise variance. This noise-isolation procedure can be mathematically described as:

$$I_{noise}^L = R_W^W - R_W^L. \quad (5)$$

In this instance, the maximum value of L is always less than or equal to W. In Fig. 8, the noise variance is plotted as a function of scale for a fixed window size of 15 pixels; we observe that there is a monotonic decrease in noise values as scale width increases.

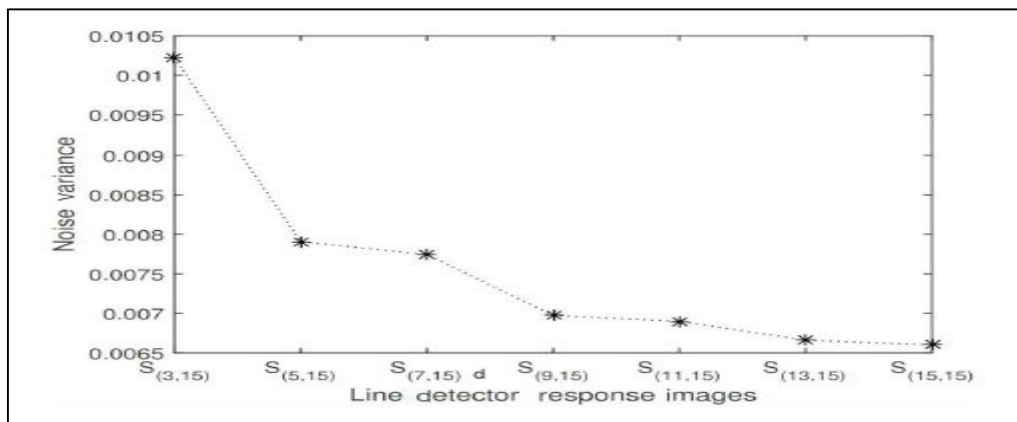Fig. 8. Noise variance of different line detectors, where S 17x17 is used as a reference.

To emphasize the variability in contributions in relation to scale images, the author in [9] adopts an ad-hoc measure whereby the weight assigned to a given scale is dependent on the line length, thus the final image is constructed as:

$$R_{combined} = \frac{1}{n_L+1}\left(\sum_L L * R_W^L + f_{avg}\right). \quad (6)$$

Since the estimated noise variance of each scale image is known, the final combined image can be computed as a weighted linear combination on a per-pixel basis. The purpose of the weighting function is to discard response images which are either too dark or too saturated, and to suppress noise by giving higher weights to response images which exhibit low noise variance. Given a sequence of independent observations, in the form of scale images R_L with noise variances σ_L, the inverse-variance weighted average is defined as per [41], that is:

$$R_{combined} = = \left(\frac{1}{n_L}\right)\frac{\sum_i \frac{R_i}{\sigma_i}}{\sum_i \frac{1}{\sigma_i}}. \qquad\qquad (7)$$

Despite the considerable noise reduction resulting from the use of the weighted average function in Eq. 7, there is still a considerable amount of background noise present in the aggregate image output. To compensate for the presence of such noise, a possible solution is to compute a weighted sum of all scale responses where the weights are based on the noise contribution made by each individual scale. It has been demonstrated that small scale filters are more affected by background noise as compared to large scale filters [9]. This research team has devised a weighting assignment protocol wherein each scale image is converted to its corresponding zero-mean and unit variance image; we then binarize the transformed image with threshold equivalent to one standard deviation above the mean to define foreground and background regions. The inverse of the variance of the background region constitutes the weight associated with the scale image. Although the aforementioned protocol does succeed in partially suppressing background noise, the problem of low-contrast pixels around vessel edges still persists because multiscale line filtering usually has the effect of blurring blood vessel edges. Nonetheless, images produced by the application of multi-scale filtering and subsequent binarization will still preserve the representations of all blood vessels present in the original image (even if the edges of said vessels are not as distinct as would be desired); moreover, it is usually the case that a filtered image – in comparison to its non-filtered counterpart – will display improved contrast with good distinction between vessel and non-vessel regions, thus making it easier to discern small blood vessels from their surrounding background.

Although the application of multi-scale line filtering will normally result in an improved representation of the vascular network under scrutiny, the resulting upgraded composite image is still not sufficiently optimized as to accommodate the imposition of global thresholding operations since there may still be a considerable degree of intra-vessel variation, i.e. cross-sectional vessel contrast is not uniform. In order, therefore, to demarcate blood vessel boundaries using thresholding techniques, this research team has implemented a modified Frangi method which executes the thresholding operation based on a ratio of eigen values. This modified Frangi method represents an improvement over the classical Frangi scheme proposed in [7] whereby a 2/3D enhancement procedure was employed to sharpen the contrast of any vessel-like structures by exploiting the relationship between eigenvectors and eigenvalues of a local Hessian matrix. In this context, the Hessian matrix would be constructed from the responses generated by a set of a second-order derivatives of the Gaussian function convolved with the image. However, the use of such second-order derivatives may be inappropriate since they are based on the assumption that blood vessels will exhibit some degree of geometrical regularity in their structure, however such regularity is not always manifested and therefore any processing technique based on Hessian second-order derivatives might produce representations of vascular structures which are fragmented and even spurious. Moreover, Frangi filters do not typically generate a uniform response for vessels of varying diameter, thus it is usually the case that Frangi filtering produces a response which is lower at vessels' edges / bifurcations compared to the response from the vessels' central regions. Moreover, the process of implementing Gaussian filter convolution with a given image tends to produce blurring of vessel boundaries, thus rendering Hessian-based scale selection unreliable. This inaccuracy is demonstrated in Eq. 8 where *I(x)* represents the intensity of the retinal image at co-ordinates $(x) = [x1;\ x2]^T$, thus the Hessian *H* of the *I(x)* at scale s is denoted by a 2 x2 matrix defined as:

$$H_{ij}((x),s) = s^2 I((x)) * \frac{\vartheta^2}{\vartheta x_i \vartheta x_j} G(X,s) \, for \, i,j = 1,2, \tag{8}$$

In this context, $G(x,s) = \frac{1}{2\pi s^2} e^{\frac{-x^2 x}{2s^2}}$, is a 2-dimensional Gaussian function and * denotes convolution. The eigenvalues of the Hessian matrix provide the required information describing the shape of the local region or object. This linear convolution is realized by sorting the eigenvalues λ_i of **H** according to their magnitudes, such that $|\lambda_1| \leq |\lambda_2|$. The most widely used Frangi enhancement filter function is:

$$if \, \lambda_2 \leq 0$$

$$v = \begin{cases} 0 \\ \exp - \left(\frac{R_B^2}{2\beta^2}\right)(1 - exp - \frac{S^2}{2C^2}) \end{cases} \tag{9}$$

It is to be noted that the term $R_B = \frac{\lambda_1}{\lambda_2}$ defines the blobness measure and $S = \sqrt{\lambda_1^2 + \lambda_2^2}$ is the second-order measure defining the structure of the image. The latter expression is dependent on the square magnitude of λ_2, which may not always be larger in magnitude at all points of the cross-sectional profile of the blood vessel under examination; this uncertainty constitutes a vulnerability that can produce incorrect computations of the blood vessel's width and structure.

In an attempt to reduce the shortcomings associated with the conventional Frangi method, research conducted by [42] proposes an improved vesselness filter based on ratio of multi-scale Hessian eigenvalues to yield a close-to-uniform response to better distinguish vascular structures from their surrounding background. Indeed, the core premise of this investigation is that it is possible to achieve a response that is not affected by variations in contrast if an enhancement function is applied which is based on a ratio of eigenvalues not directly proportional to any specific eigenvalue range. This research team is pleased to report that the results of various experimental procedures carried out during the course of the current investigation has demonstrated that the proposed enhancement operation yields a high and highly uniform response in the presence of image artifacts of varying contrast and shape.

Despite this research team's success in achieving the stated objective of generating homogeneous retinal image backgrounds and the rendering of uniform intensity for vessel cross-sections, the task of finding an appropriate threshold value remains to be resolved. In an effort to formulate a makeshift thresholding solution, we have opted for ISO-data to calculate an appropriate threshold value for generating the required binary image (wherein white pixels correspond to vascular structures while black pixels represent the background). Essentially, the ISO data extraction algorithm consists of four steps: firstly, we compute two initial mean values for the vessel and non-vessel regions, then we classify all the pixels inside the FOV region as either representing blood vessels or otherwise (such classification being dependent on the mean values of each pixel). In third step, we re-compute new mean values based on this classification. If the new mean values are substantially different from the previous ones, then the fourth step is to repeat the vessel/non-vessel pixel classification process and re-calculate the mean values arising. The thresholding calculation process is concluded when the mean values become consistent across iterations.

4. Results and Discussions

The proposed thin vessel enhancement algorithm has been evaluated via testing on retinal image corpora from two publicly available databases, namely DRIVE (available at https://www.isi.uu.nl/Research/Databases/DRIVE/) and STARE (publicly available at http://cecas.clemson.edu/ ahoover/stare/). The STARE database consists of twenty images, while the DRIVE database contains forty images which are further subdivided into an equal number of training and test images. Both databases also provide manually segmented versions of the test images which serve as "ground

truth" references for validation purposes. The performance of the proposed algorithm has been assessed by comparing its segmentation of the test images with the manually produced segmentations of the same images. For this study, the specific assessment criteria used were accuracy (Acc), sensitivity (Se) and specificity (Sp); the latter two criteria being particularly apt for providing ground truth segmentation data to distinguish blood vessels from their immediate background.

Since this paper proposes a process of enhancing thin vessels which is based on conventional multiscale line filtering [8], it is appropriate to compare our algorithm's segmentation performance with another algorithm – implemented by Nguyen [8] – that uses standard multi-scale filtering methods. This research team is pleased to report that – in terms of image segmentation results – the algorithm proposed by this research team has outperformed Nguyen's algorithm for both the DRIVE (Table 1) and STARE (Table 2) image data sets. More specifically, the new algorithm demonstrated increased sensitivity, resulting in improved detection of thinner low-contrast blood vessels.

Table 1. Sensitivity, specificity and accuracy of our modification on Nguyen [8] on DRIVE Database

gray	Sensitivity		Specificity		Accuracy	
gray	Average	Std devi.	Average	Std devi.	Average	Std devi.
Nguyen [8]	**0.7460**	0.0987	**0.9560**	0.0965	**0.9400**	0.070
Modification	**0.7696**	0.0661	**0.9651**	0.0568	**0.9506**	0.0676

Table 2: Sensitivity, specificity and accuracy of our modification on Nguyen [8] on STARE Database

gray	Sensitivity		Specificity		Accuracy	
gray	Average	Std devi.	Average	Std devi.	Average	Std devi.
Nguyen [8]	**0.7356**	0.0965	**0.9496**	0.0896	**0.9324**	0.0897
Modification	**0.7521**	0.0619	**0.9812**	0.0638	**0.9513**	0.0578

In order to evaluate the computational efficiency, we compared the time taken by the proposed algorithm vis-à-vis Nguyen's segmentation procedure to process the same fundus image. Both algorithms were implemented as source code written in the MATLAB scripting language (version 2018a) and executed on a Windows PC computer incorporating an Intel i7 processor and 16GB RAM. The proposed algorithm executed the image segmentation task in 18.0 seconds while the standard multi-scale filtering application took 10.5 seconds. It is surmised that the proposed algorithm is more computationally expensive because it incorporates an additional triple-stick filter to enhance thin blood vessels.

Table 3: Area under ROC curve for DRIVE and STARE Database

Method	DRIVE	STARE
Nguyen	0.851	0.843

Modification	0.868	0.854

In addition to comparison with Nguyen's multi-scale filtering algorithm, we have also compared the performance of our method with several recently implemented algorithms that are based on other vessel enhancement techniques. Tables 4 and 5 present the results of this comparative analysis for the test image corpora of the DRIVE and STARE databases respectively. It is to be noted that the human observer in Table 4 represents the manual segmentation data. The results shown in Table 4 indicate that the analysis adopted by Chaudhuri [20] is inherently superior compared to the other methods, however Chaudhuri's implementation does not produce the required sensitivity and accuracy. The symmetric analysis proposed by Azzopardi [41] returned a better performance for all three parameters and its specificity is higher than the method proposed by this research team; however, the sensitivity of our method is higher than all other methods for which segmentation results are available. Furthermore, our proposed method gives slightly better accuracy than even supervised methods.

Table 4: Comparison of proposed method with published methods on DRIVE database

gray gray	Sensitivity -------------------------- Average Std devi.		Specificity -------------------------- Average Std devi.		Accuracy -------------------------- Average Std devi.	
Human observer [8]	**0.7761**	0.0593	**0.9725**	0.0082	**0.9473**	0.0048
Supervised Neimeijer [34]	**0.6793**	0.0698	**0.9801**	0.0085	**0.9416**	0.0064
Unsupervised Chaudhuri [20]	**0.2716**	0.2118	**0.9794**	0.0388	**0.8894**	0.0321
Jiang [26]	**0.6478**	0.0642	**0.9625**	0.029	**0.9222**	0.0069
Zana [25]	**0.6696**	0.0764	**0.9769**	0.0079	**0.9377**	0.0077
Perez [3]	**0.7086**	0.1815	**0.9496**	0.0260	**0.9181**	0.239
ILTA[19]	**0.6960**	0.0451	**0.9416**	0.0601	**0.9100**	0.0111
MSLTA [19]	**0.7468**	0.0654	**0.9551**	0.0128	**0.9285**	0.0880
Azzopardi Symmetric [41]	**0.7526**	0.0622	**0.9707**	0.0092	**0.9427**	0.0780
Azzopardi Asymmetric [41]	**0.7696**	0.0522	**0.9621**	0.0192	**0.9422**	0.0710
Proposed	**0.7696**	0.0661	**0.9651**	0.0568	**0.9506**	0.0676

In addition to the accuracy-sensitivity-specificity evaluation criteria mentioned in the preceding paragraphs, another possible assessment protocol is the evaluation of a proposed method when performing under "worst case" conditions. To this effect, a comparison was made between our method and that of another algorithm using standard multi-scaling technology to segment an image featuring extremely noisy data (e.g. an image background of sharply varying intensity). Fig. 9 presents the segmentation output from the noisiest image of the test data set and compare these results with those produced by algorithms using standard multi-scale line filtering [8] and weighted multi-scale line filtering [9]. It is observed that the standard multi-scale method has little success in detecting blood vessels - especially the smallest vessels - under such adverse conditions. Conversely, the method proposed by this research team is better able to detect thin low-contrast blood vessels in very noisy environments.

Table 5: Comparison of proposed method with published methods on STARE database

Method	Sensitivity	Specificity	Accuracy

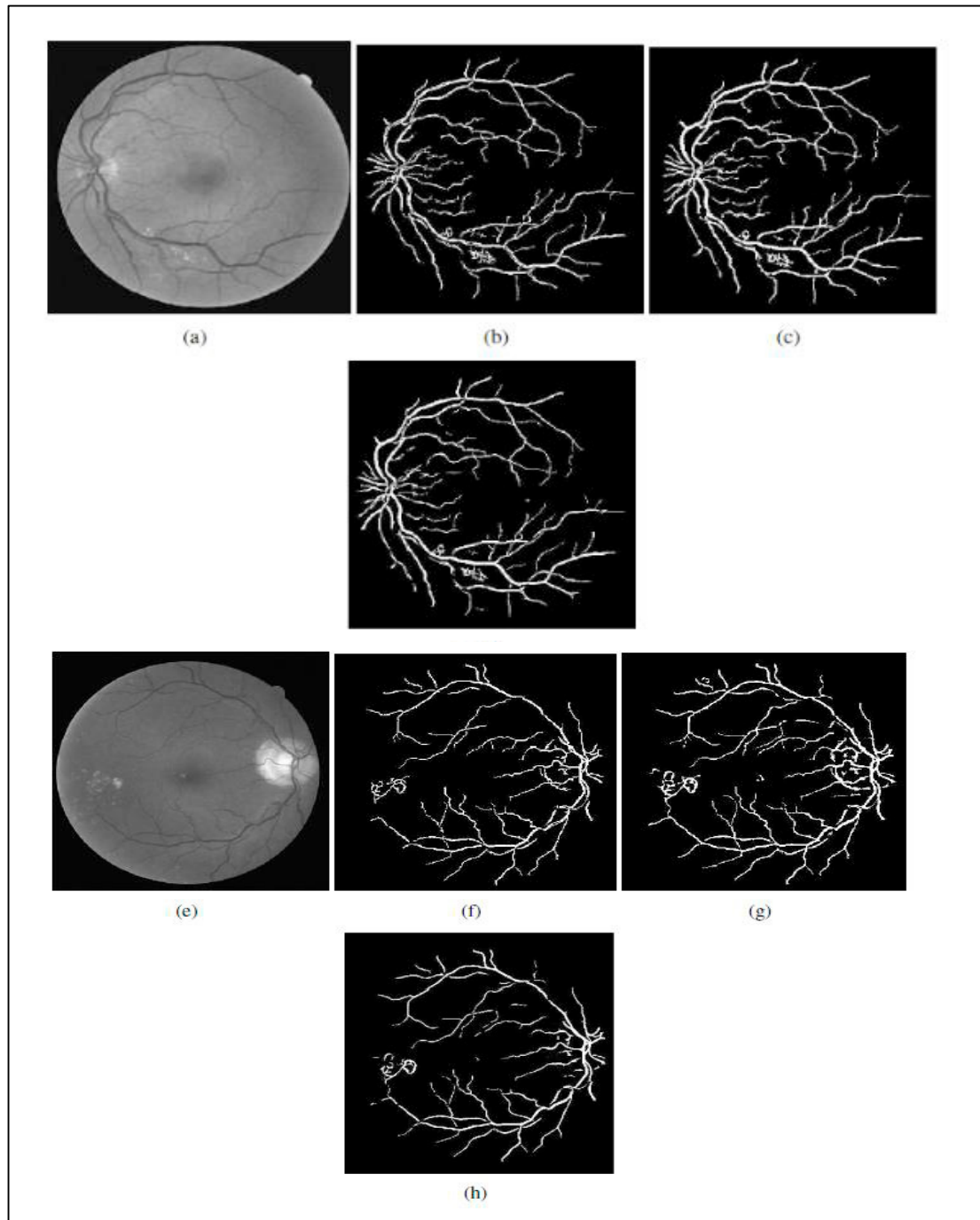| Jiang [26]	Not Given	Not Given	0.891
Azzopardi Symmetric [41]	0.7543	0.9689	0.891
Azzopardi Asymmetric [41]	0.7765	0.9742	0.943
Proposed	**0.7521**	**0.9812**	**0.9513**

Fig. 9. a) Worst sample image number :03 of DRIVE database. Outputs from b) Standard multi-scale filtering, c) Weighted multi-scale filtering, d) the proposed method. e) Worst sample image number :08 of DRIVE database. Output from f) Standard multi-scale filtering, g) Weighted multi-scale filtering, h) the proposed method.

5.   Conclusion

It is demonstrated that the retinal vascular segmentation method proposed by this research team has accomplished the hitherto elusive objective of enhancing the contrast of thin low-contrast blood vessels as well as increasing the intensity of pixels defining the edges of thicker vessels. It is also demonstrated that the proposed additional segmentation procedures can be implemented as a "plug-in" software component to boost the performance of applications using only conventional multi-scale filtering procedures to effect the segmentation of vascular networks in retinal fundus images.

References

[1] J. J.Kanski, Clinical Ophthalmology: A Systematic Approach, 7th Edition, Elsevier, 2012.

[2] D. C. Klonoff, D. M. Schwartz, An economic analysis of interventions for diabetes, Diabetes Care 23 (3) (2000) 390–404.

[3] M. E. Martinez-Perez, A. D. Hughes, A. V. Stanton, S. A. Thom, N. Chapman, A. B. Bharath, K. H. Parker, Retinal vascular tree morphology: A semi-automatic quantification, IEEE Trans. Biomed. Eng. 49 (8) (2002) 912–917.

[4] M. Niemeijer, B. van Ginneken, J. J. Staal, M. S. A. Suttorp-Schulten, M. D. Abramoff, Automatic detection of red lesions in digital color fundus photographs, IEEE Trans. Med. Imag. 24 (5) (2005) 584592.

[5] F. Zana, J. C. Klein, A multimodal registration algorithm of eye fundus images using vessels detection and hough transform, IEEE Trans. Med. Imag. 18 (5) (1999) 419428.

[6] M. M. Fraz, P. Remagnino, A. Hoppe, S. A. Barman, Retinal image analysis aimed at extraction of vascular structure using linear discriminant classifier, in: The International Conference on Computer Medical Applications, Sousse, Tunisia, 2013, pp. 1–6.

[7] E.Ricci, R.Perfetti, Retinal blood vessel segmentation using line operators and support vector classification, IEEE Trans. on Medical Images 26 (10) (2007) 13571365.

[8] U. Nguyen, A. Bhuiyan, L. Park, K. Ramamohanarao, An effective retinal blood vessel segmentation method using multi-scale line detection, Pattern Recognition 46 (2013) 703–715.

[9] Y. Hou, Automatic segmentation of retinal blood vessels based on improved multiscale line detection, Journal of Computing Science and Engineering 8 (2) (2014) 119–128.

[10] T. Jerman, F. Pernus, B. Likar, Z. Spiclin, Enhancement of vascular structures in 3d and 2d angiographic images, IEEE Transactions on Medical Imaging 35 (9) (2016) 2107–2118.

[11] A. Hunter, J. Lowell, R. Ryder, A. Basu, D. Steel, Tramline filtering for retinal vessel segmentation, in: 3rd European Medical and Biological Engineering Conference, Prague, Czech Republic, 2005, pp. 1–4.

[12] C. Xiao, M. Staring, J.Wang, D. P. Shamonin, B. C. Stoel, A derivative of stick filter for pulmonary fissure detection in CT images, in: Medical Imaging 2013: Image Processing, Vol. 8669, International Society for Optics and Photonics, 2013, p. 86690V.

[13] I.Liu, Y.Sun, Recursive tracking of vascular networks in angiograms based on the detection-deletion scheme, IEEE Trans. Med. Imaging 2 (12) (1993) 334–341.

[14] L.Zhou, M.S.Rzeszotarski, L.J.Singerman, J.M.Chokreff, The detection and quantification of retinopathy using digital angiograms, IEEE Trans. Med. Imaging 4 (13) (1994) 619–626.

[15] O.Chutatape, L.Zheng, S.Krishnan, Retinal blood vessel detection and tracking by matched gaussian and kalman filters, in: 20th Annual International Conference of the IEEE in Engineering in Medicine and Biology Society, 1998, pp. 3144–3149.

[16] Y.A.Tolias, S.M.Panas, A fuzzy vessel tracking algorithm for retinal images based on fuzzy clustering, IEEE Trans. Med. Imaging 2 (17) (1998) 263–273.

[17] A.Can, H.Shen, J.N.Turner, H.L.Tanenbaum, B.Roysam, Rapid automated tracing and feature extraction from retinal fundus images using direct exploratory algorithms, IEEE Trans. on Information Technology in Biomedicine 3 (2) (1999) 125–138.

[18] Y.Yin, M.Adel, S.Bourennane, Retinal vessel segmentation using a probabilistic tracking method, Pattern Recognition (45) (2012) 1235–1244.

[19] M.Vlachos, E.Dermatas, Multi-scale retinal vessel segmentation using line tracking, Computerized Medical Imaging and Graphics 34 (3) (2010) 213227.

[20] S.Chaudhuri, S.Chatterjee, N.Katz, M.Nelson, M.Goldbaum, Detection of blood vessels in retinal images using two-dimensional matched filters, IEEE Trans. on Med. Imaging 3 (8) (1989) 263–269.

[21] A.Hoover, V.Kouznetsova, M.Goldbaum, Locating blood vessels in retinal images by piecewise threshold probing of a matched filter response, IEEE Trans. on Med. Imaging 3 (19) (2000) 203–210.

[22] M.Al-Rawi, M.Qutaishat, M.Arrar, An improved matched filter for blood vessel detection of digital retinal images, Computers in Biology and Medicine 2 (37) (2007) 262–267.

[23] L.Zhang, Q.Li, J.You, D.Zhang, A modified matched filter with double-sided thresholding for screening proliferative diabetic retinopathy, IEEE Trans. on Information Technology in Biomedicine 4 (13) (2009) 528–534.

[24] B.Zhang, L.Zhang, F.Karray, Retinal vessel extraction by matched filter with first-order derivative of Gaussian, Computers in Biology and Medicine 4 (40) (2010) 438–445.

[25] F.Zana, J.C.Klein, Segmentation of vessel-like patterns using mathematical morphology and curvature evaluation, IEEE Trans. on Image Processing 7 (10) (2001) 1010–1019.

[26] X.Jiang, D.Mojon, Adaptive local thresholding by verification-based multi- threshold probing with application to vessel detection in retinal images, IEEE Trans. on Image Processing 25 (1) (2003) 131–137.

[27] K.Vermeer, F.Vos, H.Lemij, A.Vossepoel, A model based method for retinal blood vessel detection, Computers in Biology and Medicine 34 (3) (2004) 209–219.

[28] M.E.Martinez-Perez, A.D.Hughes, S.A.Thom, A.A.Bharath, K.H.Parker, Segmentation of blood vessels from red-free and fluorescein retinal images, Medical Image Analysis 11 (1) (2007) 47–61.

[29] B.S.Y.Lam, H.Yan, A novel vessel segmentation algorithm for pathological retina images based on the divergence of vector fields, IEEE Trans. on Medical Imaging 27 (2) (2008) 237 – 246.

[30] B.S.Y.Lam, Y.Gao, A.W.C.Liew, General retinal vessel segmentation using regularization-based multiconcavity modeling, IEEE Trans. on Medical Imaging 29 (7) (2010) 13691381.

[31] J.Staal, M.D.Abramoff, M.Niemeijer, M.A.Viergever, B.vanGinneken, Ridge-based vessel segmentation in color images of the retina, IEEE Trans. on Medical Images 23 (4) (2004) 501509.

[32] J.V.B.Soares, J.J.G.Leandro, R.M.Cesar, H.F.Jelinek, M.J.Cree, Retinal vessel segmentation using the 2-d gabor wavelet and supervised classification, IEEE Trans. on Medical Images 25 (9) (2006) 1214–1222.

[33] C.Sinthanayothin, J.F.Boyce, H.L.Cook, T.H.Williamson, Automated localisation of the optic disc,fovea,and retinal blood vessels from digital colour fundus images, British Journal of Ophthalmology 83 (8) (1999) 902.

[34] M.Niemeijer, J.Staal, B.vanGinneken, M.Loog, M.D.Abramoff, Comparative study of retinal vessel segmentation methods on a new publicly available database, Proceedings of SPIE 5370 (2004) 648656.

[35] M.Sofka, C.V.Stewart, Retinal vessel center line extraction using multiscale matched filters, confidence and edge measures, IEEE Trans. on Medical Imaging 25 (12) (2006) 15311546.

[36] C.A.Lupascu, D.Tegolo, E.Trucco, Fabc, Retinal vessel segmentation using adaboost, IEEE Trans. on Information Technology in Biomedicine 14 (5) (2010) 12671274.

[37] D.Marin, A.Aquino, M. ndez Arias, J.M.Bravo, A new supervised method for blood vessel segmentation in retinal images by using gray-level and moment invariants-based features, IEEE Trans. on Medical Imaging 30 (1) (2011) 146158.

[38] X.You, Q.Peng, Y.Yuan, Y.Cheung, J.Lei, Segmentation of retinal blood vessels using the radial projection and semi-supervised approach, Pattern Recognition 44 (2011) 23142324.

[39] J.-W. Seo, S. D. Kim, Novel pca-based color-to-gray image conversion, in: 20th IEEE International Conference on Image Processing, 2013, p. 22792283.

[40] Changyan Xiao, Marius Staring, Juan Wang, Denis P. Shamonin and Berend C. Stoel, Pulmonary Fissure Detection in CT Images using a Derivative of Stick, IEEE Transactions on Medical Imaging 35 (6) (2016) 1488-1500.

[41] G. Azzopardia, N. Strisciuglio, M. Vento, N. Petkov, Trainable COSFIRE filters for vessel delineation with application to retinal images, Medical Image Analysis 19 (1) (2015) 46–57.

[42] J. Hartung, G. Knapp, B. K. Sinha, Statistical Meta-analysis with Applications, John Wiley & Sons, 2008.